

Fermi National Accelerator Laboratory

FERMILAB-Pub-99/101-A

The Projected Three-Point Correlation Function: Theory and Observations

Joshua A. Frieman and Enrique Gaztanaga

*Fermi National Accelerator Laboratory
P.O. Box 500, Batavia, Illinois 60510*

April 1999

Submitted to *Astrophysical Journal Letters*

Disclaimer

This report was prepared as an account of work sponsored by an agency of the United States Government. Neither the United States Government nor any agency thereof, nor any of their employees, makes any warranty, expressed or implied, or assumes any legal liability or responsibility for the accuracy, completeness, or usefulness of any information, apparatus, product, or process disclosed, or represents that its use would not infringe privately owned rights. Reference herein to any specific commercial product, process, or service by trade name, trademark, manufacturer, or otherwise, does not necessarily constitute or imply its endorsement, recommendation, or favoring by the United States Government or any agency thereof. The views and opinions of authors expressed herein do not necessarily state or reflect those of the United States Government or any agency thereof.

Distribution

Approved for public release; further dissemination unlimited.

Copyright Notification

This manuscript has been authored by Universities Research Association, Inc. under contract No. DE-AC02-76CHO3000 with the U.S. Department of Energy. The United States Government and the publisher, by accepting the article for publication, acknowledges that the United States Government retains a nonexclusive, paid-up, irrevocable, worldwide license to publish or reproduce the published form of this manuscript, or allow others to do so, for United States Government Purposes.

The Projected Three-point Correlation Function: Theory and Observations

Joshua A. Frieman^{1,2} and Enrique Gaztañaga³

¹ NASA/Fermilab Astrophysics Center, Fermi National Accelerator Laboratory,
P.O. Box 500, Batavia, IL 60510

² Department of Astronomy and Astrophysics, University of Chicago, Chicago, IL 60637

³ Institut d'Estudis Espacials de Catalunya, IEEC/CSIC,
Edf. Nexus-104 - c/ Gran Capitan 2-4, 08034 Barcelona, Spain

ABSTRACT

We report results for the angular three-point galaxy correlation function in the APM survey and compare them with theoretical expectations. For the first time, these measurements extend to sufficiently large scales to probe the weakly non-linear regime. On large scales, the results are in good agreement with the predictions of non-linear cosmological perturbation theory, for a model with initially Gaussian fluctuations and linear power spectrum $P(k)$ consistent with that inferred from the APM survey. These results reinforce the conclusion that large-scale structure is driven by non-linear gravitational instability and that APM galaxies are relatively unbiased tracers of the mass on large scales; they also provide stringent constraints upon models with non-Gaussian initial conditions and strongly exclude the standard cold dark matter model.

Subject headings: cosmology: theory; cosmology: observations; cosmology:large-scale structure of universe; methods: numerical; methods: analytical

1. Introduction

Traditionally, two-point statistics, the auto-correlation function $\xi(r)$ and the power spectrum $P(k)$, have been the dominant benchmarks for testing theories of structure formation. However, with the advent of large galaxy surveys and the development of non-linear cosmological perturbation theory and large N-body simulations, it has become clear that higher-order correlations provide new probes of large-scale structure. In particular, the $N > 2$ -point functions and moments test models for bias—the relation between the galaxy and mass distributions—and constrain non-Gaussianity in the initial conditions (Fry & Gaztañaga 1993, Frieman & Gaztañaga 1994, Gaztañaga 1994, Gaztañaga & Frieman 1994, Fry 1994, Fry & Scherrer 1994, Jaffe 1994, Fry, Melott, & Shandarin 1995, Juszkiewicz, et al. 1995, Chodorowski & Bouchet 1996, Gaztañaga & Mahonen 1996, Szapudi, Meiksin, & Nichol 1996, Jing 1997, Matarrese et al. 1997, Mo, Jing, & White 1997, Verde et al. 1998, Scoccimarro et al. 1998, Scoccimarro, Couchman, & Frieman 1998).

The galaxy three-point function ζ has been measured in several angular and redshift catalogs (Peebles & Groth 1975, Peebles 1975, Groth & Peebles 1977, Fry and Seldner 1982, Bean et al. 1983, Efstathiou & Jedredjewski 1984, Hale-Sutton et al. 1989, Baumgart & Fry 1991, Jing, Mo, & Boerner 1991, Jing & Boerner 1998). Given the limited volumes covered by these surveys, these measurements generally probed the three-point function on scales $0.1 \lesssim r \lesssim 10 h^{-1}$ Mpc. They established that galaxies cluster hierarchically: on these scales, the hierarchical three-point amplitude, defined by

$$Q(x_{12}, x_{13}, x_{23}) \equiv \frac{\zeta(\mathbf{x}_1, \mathbf{x}_2, \mathbf{x}_3)}{\xi(x_{12})\xi(x_{13}) + \xi(x_{12})\xi(x_{23}) + \xi(x_{13})\xi(x_{23})}, \quad (1)$$

(with $x_{ij} = |\mathbf{x}_i - \mathbf{x}_j|$) is nearly constant, independent of scale and configuration, with values in the range $Q \simeq 0.6 - 1.3$, depending on the catalog. This hierarchical form is consistent with expectations from N-body simulations in the non-linear regime (e.g., Matsubara & Suto 1994, Fry, Melott, & Shandarin 1993, Scoccimarro et al. 1998, Scoccimarro & Frieman 1998).

On larger scales, $r \gtrsim 10 h^{-1}$ Mpc, in the weakly non-linear regime where $\xi(r) \lesssim 1$, non-linear perturbation theory (PT)—corroborated by N-body simulations—predicts that Q becomes strongly dependent on the *shape* of the triangle defined by the three points \mathbf{x}_i (Fry 1984, Fry, Melott, & Shandarin 1993, Jing & Boerner 1997, Scoccimarro 1997, Gaztañaga & Bernardeau 1998, Scoccimarro et al. 1998). The large-scale configuration-dependence of the three-point function is characteristic of the non-linear dynamics of gravitational instability and is sensitive to the initial power spectrum, to the bias, and to non-Gaussianity in the initial conditions. Thus measurement of the three-point function and its shape dependence should provide a powerful probe of structure formation models. Measurements of higher-order galaxy correlations on large scales have been confined so far to volume-averaged correlation functions—the one-point cumulants S_N —and their cousins (e.g., cumulant correlators). These statistics, based on counts-in-cells, are computationally easier to measure than the corresponding N -point functions and, being averages over many N -point configurations, can be measured with higher signal to noise as well. On the other hand, this averaging process by definition destroys the information about configuration-dependence contained in the N -point functions themselves.

In this Letter, we report measurement of the projected three-point function on large scales in the APM Galaxy Survey (Maddox et al. 1990), compare the results with predictions of non-linear perturbation theory (PT) and N-body simulations, and briefly discuss their implications for bias and non-Gaussianity.

We first recall the perturbative expression for the three-point function. To lowest order, the statistical properties of the density contrast field, $\delta(\mathbf{x}) = (\delta\rho(\mathbf{x})/\bar{\rho}) - 1$, are characterized by the auto-correlation

function $\xi(x_{12}) = \langle \delta(\mathbf{x}_1)\delta(\mathbf{x}_2) \rangle$, and its Fourier transform, the power spectrum $P(k)$, where $\langle \delta(\mathbf{k}_1)\delta(\mathbf{k}_2) \rangle = (2\pi)^3 P(k_1)\delta_D^3(\mathbf{k}_1 + \mathbf{k}_2)$; explicitly,

$$\xi(r) = \frac{1}{2\pi^2} \int dk k^2 P(k) \frac{\sin(kr)}{kr} . \quad (2)$$

In the results to be shown below, we consider the cold dark matter (CDM) family of models, with shape parameter $\Gamma = \Omega h$ ranging from 0.5 (standard CDM) to 0.2. We also consider a model consistent with the linear power spectrum inferred from the APM survey itself (Baugh & Gaztañaga 1996),

$$P_{\text{APM-like}}(k) = \frac{Ak}{[1 + (k/0.05)^2]^{1.6}} , \quad (3)$$

with k in $h \text{ Mpc}^{-1}$. For Gaussian initial conditions, to linear order in δ , the connected $N > 2$ -point functions vanish. In second-order perturbation theory, the three-point correlation function $\zeta(\mathbf{x}_1, \mathbf{x}_2, \mathbf{x}_3) \equiv \langle \delta(\mathbf{x}_1)\delta(\mathbf{x}_2)\delta(\mathbf{x}_3) \rangle$ can be expressed as (Fry 1984, Jing & Boerner 1997, Gaztañaga & Bernardeau 1998)

$$\begin{aligned} \zeta(\mathbf{x}_1, \mathbf{x}_2, \mathbf{x}_3) &= \frac{10}{7}\xi(x_{12})\xi(x_{13}) + \frac{4}{7} \left[\frac{\Phi'(x_{12})\Phi'(x_{13})}{x_{12}x_{13}} + \left(\xi(x_{12}) + 2\frac{\Phi'(x_{12})}{x_{12}} \right) \left(\xi(x_{13}) + 2\frac{\Phi'(x_{13})}{x_{13}} \right) \right] \\ &- \frac{\mathbf{x}_{12} \cdot \mathbf{x}_{13}}{x_{12}x_{13}} (\xi'(x_{12})\Phi'(x_{13}) + \xi'(x_{13})\Phi'(x_{12})) \\ &+ \frac{4}{7} \left(\frac{\mathbf{x}_{12} \cdot \mathbf{x}_{13}}{x_{12}x_{13}} \right)^2 \left(\xi(x_{12}) + 3\frac{\Phi'(x_{12})}{x_{12}} \right) \left(\xi(x_{13}) + 3\frac{\Phi'(x_{13})}{x_{13}} \right) + \text{cyclic permutations}, \end{aligned} \quad (4)$$

where

$$\Phi(r) \equiv \frac{1}{2\pi^2} \int dk P(k) \frac{\sin(kr)}{kr} , \quad (5)$$

and $f'(x) = df/dx$. In eqns.(2)-(5), the power spectrum and auto-correlation function are implicitly evaluated at linear order in perturbation theory; we expect the leading-order result (4) to be valid in the weakly non-linear regime ($\xi \ll 1$) but to break down for $\xi(r) \gtrsim 0.5$. Eqn.(4) was derived for the Einstein-de Sitter ($\Omega_m = 1$) model, but it is known to be an excellent approximation for $\Omega \gtrsim 0.1$ (Bouchet et al. 1992, 1995, Bernardeau 1994, Catelan et al. 1995, Scoccimarro et al. 1998, Kamionkowski & Buchalter 1998). For non-Gaussian initial conditions, there will in general be corrections to (4) which depend on the initial (linear) three- and four-point functions (Fry & Scherrer 1994).

The expressions above apply to unbiased tracers of the density field; since galaxies of different types (e.g., ellipticals and spirals) have different clustering properties, we know that at least some galaxy species are biased. As an example, suppose the probability of forming a luminous galaxy depends only on the underlying mean density field in its immediate vicinity. Under this simplifying assumption, the relation between the galaxy density field $\delta_g(\mathbf{x})$ and the mass density field $\delta(\mathbf{x})$ is $\delta_g(\mathbf{x}) = f(\delta(\mathbf{x})) = \sum_n b_n \delta^n$, where b_n are the bias parameters. To leading order in perturbation theory, this local bias scheme implies

$$\xi_g(x) = b_1^2 \xi(x) , \quad (6)$$

$$\zeta_g(\mathbf{x}_1, \mathbf{x}_2, \mathbf{x}_3) = b_1^3 \zeta(\mathbf{x}_1, \mathbf{x}_2, \mathbf{x}_3) + b_1^2 b_2 [\xi(x_{12})\xi(x_{13}) + \xi(x_{12})\xi(x_{23}) + \xi(x_{13})\xi(x_{23})] , \quad (7)$$

and therefore (Fry & Gaztañaga 1993, Fry 1994)

$$Q_g = \frac{1}{b_1} Q_\delta + \frac{b_2}{b_1^2} . \quad (8)$$

Gaztañaga & Frieman (1994) have used the corresponding relation for the skewness S_3 to infer $b_1 \simeq 1$, $b_2 \simeq 0$ from the APM catalog, but the results are degenerate due to the relative scale-independence of S_3 .¹ On the other hand, Fry (1994) used the projected bispectrum from the Lick catalog to infer $b_1 \simeq 3$; however, in order to extract a statistically significant Q_g from the catalog, an average over scales including those beyond the weakly non-linear regime was required. As we will see below, the configuration-dependence of Q_g on large scales in the APM catalog is quite close to that expected in PT, suggesting that b_1 is of order unity for these galaxies. The simple model above undoubtedly does not capture the full complexity of biasing (e.g., Mo & White 1996, Blanton et al. 1998, Dekel & Lahav 1998, Sheth & Lemson 1998), but it provides a convenient framework that is well matched to the quality of the current data.

In a projected catalog with radial selection function $\phi(x)$ (normalized such that $\int dx x^2 \phi(x) = 1$), the galaxy angular two- and three-point functions at small angular separations ($\theta_{ij} \ll 1$) are given by (Peebles & Groth 1975, Peebles 1980)

$$w_g(\theta) = 2 \int_0^\infty dx x^4 \phi^2(x) F^{-2}(x) \int_0^\infty du \xi_g(r; z) \quad (9)$$

$$z_g(\theta_{12}, \theta_{13}, \theta_{23}) = \int_0^\infty dx x^6 \phi^3(x) F^{-3}(x) \int_{-\infty}^\infty \int_{-\infty}^\infty dudv \zeta_g(r_{12}, r_{13}, r_{23}; z), \quad (10)$$

where θ_{12}, θ_{13} , and θ_{23} are the sides of a triangle projected on the sky. We assume the proper separations r_{ij} are small compared to the mean depth of the sample; in this case,

$$r_{ij} = \frac{1}{1+z} [(f_{ij}/F)^2 + x^2 \theta_{ij}^2]^{1/2}, \quad (11)$$

with $f_{12} = u$, $f_{13} = v$, and $f_{23} = u - v$. Here, x is the comoving radial (coordinate) distance to redshift z , and $F(x, \Omega)$ is a geometrical factor which relates proper and coordinate distance intervals, $F(x) = [1 - (H_0 x/c)^2 (\Omega - 1)]^{1/2}$.

The radial selection function for the APM Galaxy Survey can be approximated by (Gaztañaga & Baugh 1998)

$$\phi(x)_{APM} = C x^{-b} e^{-x^2/D^2}, \quad (12)$$

with $b = 0.1$ and $D = 335 h^{-1}$ Mpc. At this depth, to an accuracy of better than a few percent we can approximate F by its Einstein-de Sitter value $F = 1$. The projected hierarchical amplitude is defined by analogy with eqn.(1),

$$q_3(\theta_{12}, \theta_{13}, \theta_{23}) \equiv \frac{z_g(\theta_{12}, \theta_{13}, \theta_{23})}{w_g(\theta_{12})w_g(\theta_{13}) + w_g(\theta_{12})w_g(\theta_{23}) + w_g(\theta_{13})w_g(\theta_{23})}. \quad (13)$$

In projecting eqns.(2) and (4) in PT we assume leading-order perturbative growth for the redshift-evolution of ξ and ζ for $\Omega_m = 1$; in this case, both Q and q_3 are independent of the power spectrum normalization (e.g., independent of σ_8).

For the analysis, we use the equal-area projection pixel map of the APM survey, with an area roughly $120^\circ \times 60^\circ$, containing $N_{gal} \simeq 1.3 \times 10^6$ galaxies brighter than $b_j = 20$ and fainter than $b_j = 17$. Each pixel has an area $(\Theta_p)^2 \simeq (0.06)^2$ sq. deg., and the mean galaxy count per pixel is $\langle N \rangle = N_{gal}/N_{pix} = 0.97$. The

¹Bernardeau (1995) pointed out a systematic correction to the way the S_J predictions should be projected. After taking into account the correct selection function and the uncertainties in the APM shape of $P(k)$, this effect is less significant than claimed by Bernardeau, and the original interpretation is still valid, in agreement with the results for q_3 presented here.

estimator of the density fluctuation amplitude at the i th pixel is $\hat{\delta}_i = (N_i/\langle N \rangle) - 1$, where N_i is the galaxy count in that pixel. The estimator for the galaxy angular two-point function is then (Peebles & Groth 1975)

$$\hat{w}(\theta) = \frac{1}{N_\theta^{(2)}} \sum_{i,j} \delta_i \delta_j W_{ij}(\theta), \quad (14)$$

where $N_\theta^{(2)} = \sum_{i,j} W_{ij}(\theta)$ is the number of pairs of pixels at separation θ in the survey region, and the angular window function $W_{ij}(\theta) = 1$ if pixels i and j are separated by $|\vec{\theta}_i - \vec{\theta}_j| = \theta \pm \Theta_p$, and 0 otherwise. The reduced angular three-point function is estimated as

$$\hat{z}(\theta_{12}, \theta_{13}, \theta_{23}) = \frac{1}{N_\theta^{(3)}} \sum_{i,j,k} \delta_i \delta_j \delta_k W_{ijk}(\theta_{12}, \theta_{13}, \theta_{23}), \quad (15)$$

where $N_\theta^{(3)} = \sum_{i,j,k} W_{ijk}$ is the count of triplets of pixels with angular separations $\theta_{12}, \theta_{13}, \theta_{23}$ in the survey region, and $W_{ijk} = 1$ for pixel triplets with that angular configuration and 0 otherwise. We note that, in the limit of counts of pairs and triplets of objects, these estimators are equivalent to the minimum variance estimators of Landy & Szalay (1993) and Szapudi & Szalay (1998). We employ these estimators for angular separations ≥ 0.5 deg, at least an order of magnitude larger than the pixel scale; in this limit, finite pixel-size corrections should be less than a few percent and have been neglected.

To test the validity of PT on the scales of interest, to verify the algorithm for measuring the angular three-point function, and to check projection and finite sampling (and boundary) effects in the APM survey, we use the simulated APM maps of Gaztañaga & Baugh 1998. These are created from N-body simulations of the SCDM (with $\sigma_8 = 1$) and APM-like ($\sigma_8 = 0.8$) models, with box size of $600 h^{-1}$ Mpc and 128^3 particles, both with $\Omega_m = 1$. From each N-body realization we make 5 APM-like maps from 5 different observers; the observers are spaced sufficiently far apart compared to D that the ‘galaxies’ they observe do not appear to be strongly correlated (Gaztañaga & Bernardeau 1998). As the simulation is done in a periodic box, we replicate the box to cover the full radial extent of the APM (around $1800 h^{-1}$ Mpc, at which distance the expected number of galaxies is smaller than unity). To account for possible boundary effects, we employ the APM angular survey mask, including plate shapes and holes. We have also made larger angular maps without the APM mask and find no significant differences from the results shown below, from which we conclude that the APM mask does not affect the estimations of the 2 or 3-point functions on the scales under study here. The projected simulations have $\sim 30\%$ lower mean surface density of galaxies than the APM. We have diluted the APM pixel maps by this amount (by randomly sampling the galaxies) and found that this dilution has a negligible effect on the clustering properties within the errors.

To estimate the projected 3-point function we need to find all triplets in the pixel maps which have a given triangle configuration and repeat the process for all configurations. Consider a triplet of pixels with labels 1,2,3 on the sky. Let θ_{12} and θ_{13} be the angular separations between the corresponding pairs of pixels and α the interior angle between these two triangle sides. One can characterize the configuration-dependence of the three-point function by studying the behavior of $q_3(\alpha)$ for fixed θ_{12} and θ_{13} . Our algorithm for counting such triplets is as follows. For each pixel in the map, we find all pixels that lie in two concentric annuli of radii $\theta_{12} \pm 0.5$ and $\theta_{13} \pm 0.5$ about it, where θ_{ij} is now measured in units of Θ_p . We count all pairs of pixels between the two annuli; this requires $(m_{12} \times m_{13})/2$ operations, where $m_{ij} = 2\pi\theta_{ij}$. As seen from the central pixel, each pair has an angular separation α , and the results are binned in α . We repeat this procedure for each pixel in the map, building the estimators (14) and (15). Thus, to find all triplets with separations θ_{12} and θ_{13} requires only $N_{pix}(m_{12} \times m_{13})/2$ operations; for $\theta_{12} = \theta_{13} = 1$ deg, this computation only takes a few hours of CPU time on a modest workstation. By contrast, a naive $\mathcal{O}(N_{pix}^3)$ operation with $N_{pix} \simeq 10^6$ would be quite a lengthy computational task given current computer power.

The two lower panels in Fig. 1 show results for $q_3(\alpha)$ for the SCDM and APM-like models, for $\theta_{12} = \theta_{13} = 2$ degrees, projected at the depth of the APM survey. The configuration-dependence of the hierarchical three-point amplitude is seen to be quite sensitive to the shape of the power spectrum. Both the shape and amplitude of $q_3(\alpha)$ predicted by PT (solid curves) are reproduced by the N-body results (points) even on these moderately small scales (at the mean depth of the APM, 2 deg corresponds to $\simeq 14 \text{ h}^{-1} \text{ Mpc}$). Part of this agreement traces to the fact that q_3 involves a weighted sum over spatial 3-point configurations covering a range of scales; due to the shape of the power spectrum, Q increases on large scales, so these configurations (which are further in the perturbative regime) are more heavily weighted in projection. The error bars on the simulation results are estimated from the variance between 10 maps (5 observers each in 2 N-body realizations), assuming they are independent, and correspond to the $1\text{-}\sigma$ interval of confidence for a single observer (i.e., they are not divided by $\sqrt{10-1}$).

The top panel of Fig. 1 and all those of Fig. 2 show the measurements of $q_3(\alpha)$ in the APM survey itself at $\theta_{12} = \theta_{13} = 0.5 - 4.5$ degrees. Closed squares correspond to estimations in the full APM map. The values at $\alpha = 0$ are in agreement with the cumulant correlators, $c_{12} \equiv q(0)$, estimated (with 4×4 bigger pixels) by Szapudi & Szalay (1999). The mean values are comparable to the values of $s_3/3$ in the APM (Gaztanaga 1994, Szapudi et al. 1995). Also notice that at the scales considered here, ≥ 0.5 deg, the values of s_3 in the APM and the EDSGC (Szapudi, Meiksin, & Nichol 1996) are very similar (Szapudi & Gaztanaga 1998).

The APM results are compared with the values of q_3 for the APM-like spectrum in PT (solid curves) and in simulations (open triangles with errorbars). As the APM-like model has, by construction, the same $w(\theta)$ as the real APM map, we assume that the sampling errors should be similar in the APM and in the simulations. This might not be true on the largest scales, however, where systematics in both the APM survey and the simulations are more important (e.g., the simulation might be affected by the periodic boundaries, and the power in the simulation and in the survey may differ on the largest scales). At scales $\theta \gtrsim 1$ deg, the agreement between the APM-like model and the APM survey is quite good; this corresponds roughly to physical scales $r \gtrsim 7 \text{ h}^{-1} \text{ Mpc}$, not far from the non-linear scale (where $\xi_2 \simeq 1$). At 4.5 deg, the APM agrees better with the PT prediction than with the simulation results, which show large variance; this could be an indication that the $600 \text{ h}^{-1} \text{ Mpc}$ simulation box is not big enough, leading to larger sampling errors than the APM itself. We also note that the SCDM model clearly disagrees with the APM data for q_3 ; this can be seen at $\theta_{12} = \theta_{13} = 2$ deg (Fig.1) and for $\theta_{12} = \theta_{13} = 3.5$ deg (dashed curve in lower-left panel of Fig. 2). This conclusion is independent of the power spectrum normalization.

At smaller angles, $\theta \lesssim 1$ deg, q_3 in the simulations is larger than in either the real APM or PT (top-left panel in Fig. 2). The discrepancy between simulations and PT on these relatively small scales is clearly due to non-linear evolution. The interpretation of the discrepancy with the real APM is less clear: a number of assumptions underlying the simulations could affect the final results at these non-linear scales. For example, systematic uncertainties in the APM selection function or a linear bias would lead one to infer a different linear APM-like power spectrum from the $w(\theta)$ data. Also, a model with low Ω_m would undergo less non-linear evolution, which might give a better match to the APM results for q_3 ; this could provide an interesting test for a low-density universe. This discrepancy at non-linear scales is similar to the one found in Baugh & Gaztañaga (1996), where the real APM values of S_J were closer to the PT predictions than to simulations. Other possible contributions to this effect include non-linear bias and non-linear projection effects (Gaztañaga & Bernardeau 1998).

The open circles in each figure show the mean of the estimations of q_3 in 4 disjoint subsamples of the APM survey (equally spaced in right ascension, as in Baugh & Efstathiou 1994). For illustration, the values of q_3 for each of the 4 zones are shown in the top panel of Figure 1: the dotted, short-dashed, long-dashed,

and dot-dashed curves correspond to zones of increasing RA (the middle two of these correspond to relatively lower galactic latitude). These estimations of q_3 are subject to larger finite-volume effects, because each zone is only 1/4 the size of the full APM. Because the zones cover a range of galactic latitude, a number of the systematic errors in the APM catalog (star-galaxy separation, obscuration by the galaxy, plate matching errors) might be expected to vary from zone to zone. We find no evidence for such systematic variation in q_3 : the individual zone values are compatible with the full survey within the (sampling) errors in the simulations (compare the top and middle panels in Figure 1). On larger scales, $\theta \gtrsim 3$ deg, the individual zone amplitudes exhibit large variance, and boundary effects come into play.

On all scales, we find large covariance between the errors of q_3 : the data points at different α are strongly correlated. This is illustrated in the middle panel of Fig. 1: the dotted and continuous curves correspond to results for 2 of the 10 observers. Sampling or finite-volume effects are seen to produce a systematic vertical shift in the curve rather than a scatter around some mean value. A similar trend is found in the real APM catalog (compare the 4 curves in the top panel of Fig. 1). This covariance can be studied analytically (Hui, Scoccimarro, Frieman, & Gaztanaga, in preparation) and comes from fluctuations on scales comparable to the sample size. Ratio bias and integral-constraint bias (e.g., Hui & Gaztanaga 1999) could also be important.

Other possible sources of systematic discrepancies between the model predictions and the APM results include the shape of the APM radial selection function, the evolution of clustering, and the shape of the linear power spectrum. We find that the first two effects introduce differences smaller than 10% in the amplitude of q_3 (in agreement with Gaztanaga 1995), which are not significant given the errors. The uncertainty in the shape of the linear $P(k)$ is more important, and as mentioned above is critical for the interpretation of q_3 at the smallest angles. Nevertheless, at large scales ($\theta > 1$ deg) these uncertainties appear to be within the errors (when we take into account that the errors are strongly correlated). This is illustrated in the bottom-left panel of Fig. 2—the two solid curves bracketing the APM-like results show the PT predictions for two power spectra which conservatively bracket the uncertainties in the linear spectrum inferred from the APM $w(\theta)$ (see Fig.13 of Gaztanaga & Baugh 1998): $P(k) \sim k^a/[1 + (k/0.06)^3]$, with $a = 0.2$ and 1.2 . The model with $a = 1.2$ (the lower solid curve at small α) appears to give a better match to the q_3 results in the APM than the central APM-like model of Eq.[3]; for reference, a CDM model with $\Gamma = 0.3$ gives a nearly identical value for $q_3(\alpha)$ on these scales. Thus, although the APM results for q_3 generally fall below the PT predictions on angular scales $\theta \gtrsim 2$ deg, they are consistent within the sampling errors and given the uncertainties in the shape of the linear power spectrum inferred from the APM $w(\theta)$.

To place accurate constraints upon bias models and initially non-Gaussian fluctuations, we must quantitatively model the covariance between the estimates of q_3 ; this will be done elsewhere, but we can nevertheless get a qualitative sense of the limits here. We expect the strongest constraints to come from intermediate scales, $\theta \simeq 1 - 2.5$ deg, where both the sampling errors and the non-linearities are small. The upper right panel of Fig. 2 shows the PT predictions for the APM-like model with linear bias parameter $b_1 = 2$ (dashed curve) and a non-linear bias model with $b_1 = 1$, $b_2 = -0.5$ (dotted curve). Even if the errors are 100% correlated, these models are clearly ruled out by the APM data; we conservatively conclude that $b_1 \lesssim 1.5$ is required for a simple linear bias model to fit the APM data. Note that a model with $b_1 = 1.5$ and $b_2 = 0.5$ would have roughly the correct amplitude for q_3 , but its shape would be flatter than the data, especially at larger θ .

As a simple example of a non-Gaussian model, the dotted curve in the lower-left panel of Fig. 2 shows the leading-order prediction for the χ^2 isocurvature model (Peebles 1997, 1998a, 1998b, Antoniadis, et al. 1997, Linde & Mukhanov 1997, White 1998) with the APM-like spectrum. In this model, the initial

density field is the square of a Gaussian random field, and the leading-order 3-point function is simply $\zeta = 2[2\xi(x_{12})\xi(x_{13})\xi(x_{23})]^{1/2}$. Clearly, the projected three-point function for this model is substantially larger than that of the corresponding Gaussian model for intermediate α ; both the amplitude and shape are discrepant with the APM data. To make this comparison precise, the non-linear corrections for this model should be self-consistently included; however, these corrections are expected to increase rather than reduce the q_3 amplitude, likely making the disagreement worse. In general, if we assume no biasing, the initial non-gaussianities are restricted to $|q_3| \lesssim 0.5$.

At angular scales $\theta \gtrsim 1$ deg, corresponding to physical scales for which $\xi \lesssim 1$, the agreement between PT and the APM survey for the angular three-point amplitude q_3 is quite good, implying that APM galaxies are not significantly biased on these scales and that their spatial distribution is consistent with non-linear evolution from Gaussian initial conditions. This substantiates and extends the conclusions of Gaztañaga (1994,1995) and Gaztañaga & Frieman (1994).

We thank A. Buchalter, A. Jaffe, and M. Kamionkowski, who have recently carried out an independent computation of the angular three-point function in PT, for discussions, as well as L. Hui, R. Juszkiewicz, and R. Scoccimarro. EG would like to thank G.Dalton, G.Efstathiou and the Astrophysics group at Oxford, where this work started. This research was supported in part by the DOE and by NASA grant NAG5-7092 at Fermilab and by NATO Collaborative Research Grants Programme CRG970144 between IEEC and Fermilab. EG also acknowledges support by IEEC/CSIC and by DGES(MEC) (Spain), project PB96-0925.

REFERENCES

- Antoniadis, I., Mazur, P.O., & Mottola, E. 1997, Phys. Rev. Lett., 79, 14
- Baugh, C., & Gaztañaga, E. 1996, MNRAS, 280, L37
- Baumgart, D. J. & Fry, J. N. 1991, ApJ, 375, 25
- Bean, A. J., Efstathiou, G., Ellis, R. S., Peterson, B. A., & Shanks, T. 1983, MNRAS, 205, 605
- Bernardeau, F. 1994, ApJ, 433, 1
- Bernardeau, F. 1995, A&A, 301, 309
- Blanton, M., Cen, R., Ostriker, J., & Strauss, M. 1998, astro-ph/9807029
- Boschán, P., Szapudi, I., & Szalay, A. S. 1994, ApJS, 93, 65
- Bouchet, F. R., Juszkiewicz, R., Colombi, S., & Pellat, R. 1992, ApJ,394,L5
- Bouchet, F. R., Colombi, S., Hivon, E., & Juszkiewicz, R. 1995, A & A, 296, 575
- Catelan, P., Lucchin, F., Matarrese, S., & Moscardini, L. 1995, MNRAS, 276, 39
- Chodorowski, M. & Bouchet, F. 1996, MNRAS, 279, 557
- Dekel, A., & Lahav, O. 1998, astro-ph/9806193
- Efstathiou, G. & Jedredjewski, R. I. 1984, Adv Space Res, 3, 379

- Frieman, J. A., & Gaztañaga, E. 1994, ApJ, 425, 392
- Fry, J. N. 1984, ApJ, 279, 499
- Fry, J. N. 1994, Phys Rev Lett, 73, 215
- Fry, J. N. & Gaztañaga, E. 1993, ApJ, 413, 447
- Fry, J. N., Melott, A. L. & Shandarin, S. F. 1993, ApJ, 412, 504
- Fry, J. N., Melott, A. L. & Shandarin, S. F. 1995, MNRAS, 274, 745
- Fry, J. N. & Scherrer, R. 1994, ApJ, 429, 36
- Fry, J. N. & Seldner, M. 1982, ApJ, 259, 474
- Gaztañaga, E. 1994, MNRAS, 268, 913
- Gaztañaga, E. 1995, MNRAS, 454, 561
- Gaztañaga, E. & Baugh, C. 1998, MNRAS, 294, 229
- Gaztañaga, E. & Bernardeau, F. 1998, A & A, 331, 829
- Gaztañaga, E. & Frieman, J. A., 1994, ApJ, 437, L13
- Gaztañaga, E. & Mahonen, P. 1996, ApJ, 462, L1
- Groth, E. J. & Peebles, P. J. E. 1977, ApJ, 217, 385
- Hale-Sutton, D., Fong, R., Metcalfe, N., & Shanks, T. 1989, MNRAS, 237, 569
- Jaffe, A. 1994, Phys. Rev. D, 49, 3893
- Jing, Y. P. 1997, in “Cosmological parameters and the evolution of the Universe,” Proc. of IAU Symposium 183
- Jing, Y. P. & Boerner, G. 1997, A & A, 318, 667
- Jing, Y. P. & Boerner, G. 1998, ApJ, 503, 37
- Jing, Y. P., Mo, H., & Boerner, G. 1991, A & A, 252, 449
- Juszkiewicz, R., Bouchet, F., & Colombi, S. 1993, ApJ, 412, L9
- Juszkiewicz, R., Weinberg, D. H., Amsterdamski, P., Chodorowski, M., & Bouchet, F. 1995, ApJ, 442, 39
- Kamionkowski, M. & Buchalter, A. 1998, ApJ, in press
- Landy, S. D., & Szalay, A. S. 1993, ApJ, 412, 64
- Linde, A. & Mukhanov, V. 1997, Phys. Rev. D, 56, 535
- Maddox, S. J., Efstathiou, G., Sutherland, W. J., & Loveday, J. 1990, MNRAS, 242, 43P
- Matarrese, S., Verde, L., & Heavens, A. F. 1997, MNRAS, 290, 651

- Mo, H., Jing, Y. P., & White, S. D. M. 1997, MNRAS, 284, 189
- Mo, H., & White, S. D. M. 1996, MNRAS, 282, 317
- Peebles, P. J. E. 1975, ApJ, 196, 647
- Peebles, P. J. E. 1980, *The Large Scale Structure of the Universe*, Princeton: Princeton University Press
- Peebles, P. J. E. 1997, ApJ, 483, L1
- Peebles, P. J. E. 1998a, astro-ph/9805194
- Peebles, P. J. E. 1998b, astro-ph/9805212
- Peebles, P. J. E. & Groth, E. J. 1975, ApJ, 196, 1
- Scoccimarro, R. 1997, ApJ, 487, 1
- Scoccimarro, R., Colombi, S., Fry, J. N., Frieman, J., Hivon, E., & Melott, A. 1998, ApJ, 496, 586
- Scoccimarro, R., Couchman, H., & Frieman, J. 1998, astro-ph/9808305, to appear in ApJ
- Scoccimarro, R. & Frieman, J. 1998, astro-ph/9811184
- Sheth, R., & Lemson, G. 1998, astro-ph/9808138
- Szapudi, I., Dalton, G.B., Efstathiou, G. & Szalay, A. S. 1995, ApJ, 444, 520
- Szapudi, I., Meiksin, A., & Nichol, R. C. 1996, ApJ, 473, 15
- Szapudi, I., & Szalay, A. S. 1998, ApJ, 494, L41
- Szapudi, I., & Szalay, A. S. 1999, ApJ, 515, L43
- Szapudi, I., & Gaztanaga, E. 1998, MNRAS, 300, 493
- Verde, L., Heavens, A., & Matarrese, S. 1998, MNRAS, 300, 747
- White, M. 1998, astro-ph/9811227

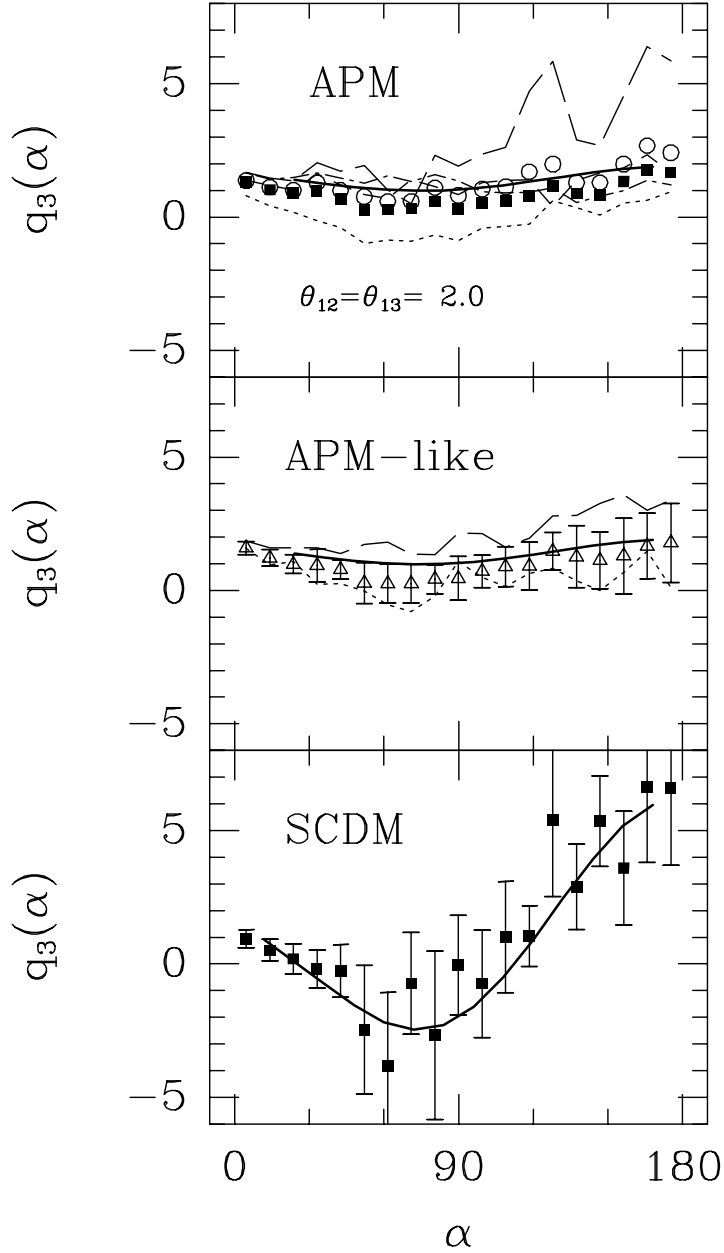


Fig. 1.— The two lower panels show perturbation theory predictions (solid curves) and N-body results (points with sampling errors) for the projected 3-point amplitude $q_3(\alpha)$ at fixed $\theta_{12} = \theta_{13} = 2$ deg for a survey with the APM selection function. N-body results are the mean from 10 observers. Middle panel corresponds to the initial APM-like power spectrum of Eqn.(3) and lower panel to the SCDM model. Additional curves in the middle panel show results for two different observers. The top panel compares the PT prediction for the APM-like model with the real APM measurements (closed squares and open circles correspond to the full APM map and to the mean of 4 zones; other curves in the top panel show results for each of the zones).

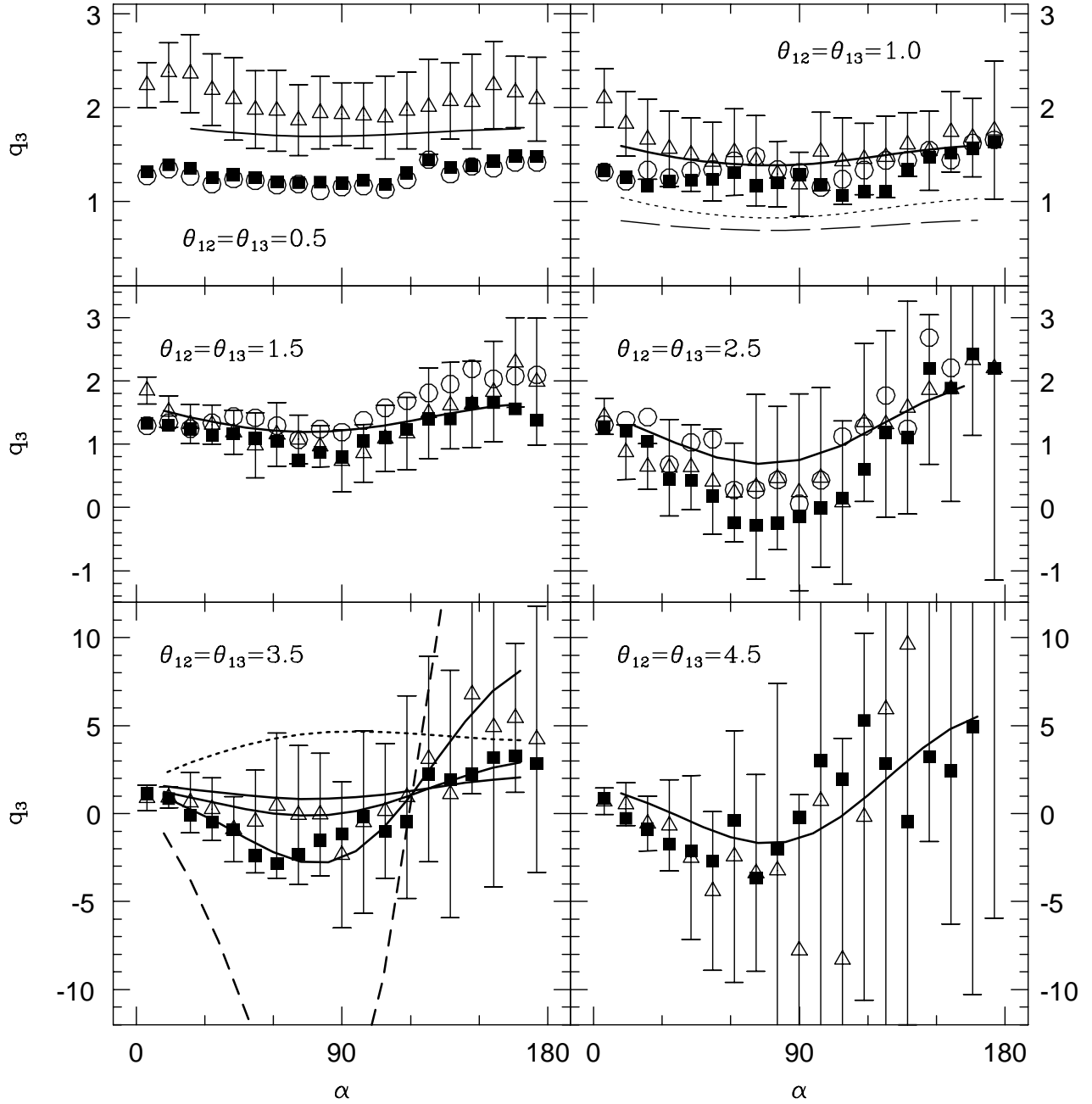


Fig. 2.— The projected 3-point amplitude q_3 in PT (solid curves) and N-body results (open triangles with errorbars) for the APM-like power spectrum are compared with q_3 measured in the APM survey (closed squares and open circles, with same meanings as in Fig. 1). Each panel shows the amplitude at different $\theta_{12} = \theta_{13}$. In upper right panel, dotted and dashed curves correspond to PT predictions with $b_1 = 1, b_2 = -0.5$ and $b_1 = 2, b_2 = 0$, respectively. In the lower left panel, upper and lower solid curves conservatively bracket the uncertainties in the inferred APM-like power spectrum, long-dashed curve corresponds to SCDM, and the dotted curve shows the leading-order prediction for the χ^2 non-Gaussian model.